2018 IEEE/RSJ International Conference on Intelligent Robots and Systems (IROS)
Madrid, Spain, October 1-5, 2018

Ladder Climbing with a Snake Robot

Tatsuya Takemori, Motoyasu Tanaka, and Fumitoshi Matsuno

Abstract— **This paper presents a method that allows a snake robot to climb a ladder. We propose a ladder climbing method for a snake robot that has a smooth surface shape. We design a novel gait for the snake using a gait design method that configures the target form of the snake robot by connecting simple shapes. The climbing motion is executed via shift control and the corresponding motion required to catch the next step on the ladder. In addition, we developed a snake robot that has a smooth exterior body surface through construction of pectinate-shaped parts of the links. We demonstrated the effectiveness of both the proposed gait and the design of the snake robot experimentally.**

I. Introduction

While snakes have simple body forms without limbs, they can realize a wide range of motions, including movements on rough terrain, sandy ground, and trees. A snake robot, which is an engineered application based on the mechanism of a snake, is intended to perform a wide variety of tasks using a simple structure. It is expected that snake robots will be used in rescue activities and in infrastructure inspection applications. To realize such practical implementations, it is necessary to expand the range of environments in which snake robots can move, and methods of controlling snake robots have been studied extensively.

Hirose [1] first used passive wheels to mimic the anisotropy of friction and realized propulsion of their snake by creating a snake robot that had passive wheeled links connected in series using active joints. Subsequently, by alternately combining pitch joints and yaw joints, the motion of their snake robot was expanded into three dimensions. Tanaka et al [2] proposed a control method that used a kinematic model to track the trajectory of a wheeled snake robot on steps. This type of method, which used a model of the interaction between the snake robot and its environment, is effective for use in a simple environment such as a plane.

However, this model-based control method cannot be applied to unknown irregular environments. Therefore, it is more effective to control the whole form of a snake robot based on its previously designed form when operating in an irregular environment. While such a control method cannot be designed based on kinematic or dynamic optimization, it is useful for application to a complex environment that cannot be modeled. To enable control of the entire form of the snake robot, some gait functions were proposed, including *sidewinding* and *helical rolling*. A gait function defines the trajectory of a joint angle in the form of a parameterized equation [3], [4]. Using gait functions, the form of the snake robot can be controlled using only a few parameters with clear physical meanings. Rollinson and Choset [4] proposed a method to estimate the entire form of a robot in a space using its gait parameters based on the current joint angle with an extended Kalman filter. Using this method, they realized autonomous movement of the robot on a pipe with a diameter that changed continuously and semi-autonomous movement on a bent pipe. However, it is difficult to formulate the joint angles directly as a function of the gait to realize the more complex target form of the snake robot.

To realize the more complex form required, a method of approximating the form of a snake robot into a target form that can be expressed as a continuous spatial curve has been studied previously [5]–[11]. Using this method, the form of a snake robot can be considered in an abstract manner as a continuous curve and there is thus no need to determine the joint angles directly, which then makes it easy to design a complex form. Yamada et al. modeled the form of a snake robot using the Frenet–Serret formulas [7] and proposed a method to derive suitable joint angles based on the curvature and the torsion of the target curve [8]. This method has only a small calculation load and is easy to perform. Using Yamada's method [8], various snake robot gaits have been proposed [9]–[11]. Kamegawa realized *bending helical rolling* [9] with a target form that is designed by connecting a helix to a shape called the *bending helix* for propulsion along a bending pipe. Qi et al. [10] proposed a method to move across a branch on a pipe by designing wave propagation motion superimposed on a helical form. Zhen et al. [11] proposed a *rolling hump* with a target form that is a curve designed by superimposing an arc-shaped curve with hump-shaped curves. This gait makes it possible for a snake robot to move over an obstacle on the ground by simply lifting the body of the snake robot locally.

However, it becomes increasingly difficult to express more complex target forms analytically. There is also the problem that the torsion sometimes becomes infinite if there are regions of zero curvature within a target form [7]. To solve these problems, we proposed a method [12] to represent a target form by connecting simple shapes such as straight lines, circular arcs, and helixes and fitting the snake robot form to the target form. Using this method, we can design the target form intuitively as a combination of segments of

This work was partially supported by the ImPACT Program of the Council for Science, Technology and Innovation (Cabinet Office, Government of Japan).

T. Takemori and F. Matsuno are with the Department of Mechanical Engineering and Science, Graduate School of Engineering, Kyoto University, Kyoto, 606-8501, Japan takemori.tatsuya.23a@st.kyoto-u.ac.jp, matsuno@me.kyoto-u.ac.jp

M. Tanaka is with the Department of Mechanical and Intelligent Systems Engineering, The University of Electro-Communications, Tokyo 182-8585, Japan mtanaka@uec.ac.jp

Authorized licensed use limited to: Hainan University. Downloaded on February 10,2025 at 12:26:22 UTC from IEEE Xplore. Restrictions apply.

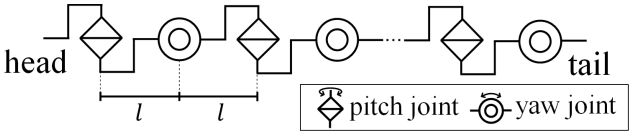

Fig. 1. Structure of the snake robot.

simple shapes with clear geometric characteristics. We used the method to design two gaits for a snake robot [12]. The first is the gait required to climb over a flange on a pipe. The second is the *crawler gait*, which allows propulsion over rough terrain.

It is necessary to design an effective gait to extend the range of environments in which the snake robot can be used. By realizing a ladder climbing motion, the areas that the snake robot can reach are extended to a much wider extent in the vertical direction. On the ladder, where there are few contact points between the snake robot and its environment, a special motion is needed to climb without falling. In this paper, we propose a novel gait for a snake robot to allow it to climb a ladder and present the mechanical design of a snake robot to realize the ladder climbing motion. We design the target form of the robot using the method of connecting simple shapes [12] and the motion used to climb the ladder is based on shift control. In addition, even if this motion is applied to a tethered snake robot, the cable will not become caught in the ladder. To demonstrate the proposed method, we have developed a novel snake robot with a smooth exterior body surface. The smoothness of the body surface is important because it allows the robot to propel itself without becoming stuck in the environment.

This research is based on [13] and is improved by adding the expansion of the gait to an inclined ladder, design and development of the snake robot, and conducting experiments.

II. Gait Design and Fitting Method

A. Shape Fitting Using the Backbone Curve

We use a snake robot model that is composed of alternately connected pitch-axis and yaw-axis joints, as shown in Fig. 1. The number of joints is represented by n_{joint} and the link length is l. The upper value of the absolute angle of a joint is $\theta_{\max}$.

In this section, we explain the method used to express the target form of the snake robot and approximate the form of a snake robot to this target form. This method involves two steps. The first step is to obtain the relationship between the *Frenet–Serret frame* and the *backbone curve* [14]. The second step is to calculate the desired joint angles to allow the form of the snake robot to be fitted to the target form. We used Yamada's approximation method [8] to perform the second step because it has low computational cost and can easily be applied when the curvature and the torsion of the target form are known.

1) First Step: In this step, we consider the relationship between the *Frenet–Serret frame* and the *backbone curve*, which is used to express the target form of the snake robot.

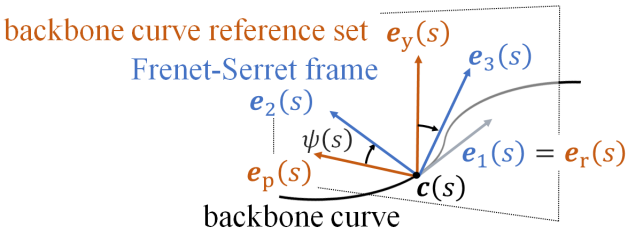

Fig. 2. Difference between the Frenet–Serret frame and the backbone curve reference set.

A general spatial continuum curve $\boldsymbol{c}(s)$ is expressed using the Frenet-Serret equation with curvature $\kappa(s)$ and torsion $\tau(s)$, as follows:

$$\begin{cases} \mathrm{d}\boldsymbol{c}(s)/\mathrm{d}s &= \boldsymbol{e}_1(s) \\ \mathrm{d}\boldsymbol{e}_1(s)/\mathrm{d}s &= \kappa(s)\boldsymbol{e}_2(s) \\ \mathrm{d}\boldsymbol{e}_2(s)/\mathrm{d}s &= -\kappa(s)\boldsymbol{e}_1(s) + \tau(s)\boldsymbol{e}_3(s) \\ \mathrm{d}\boldsymbol{e}_3(s)/\mathrm{d}s &= -\tau(s)\boldsymbol{e}_2(s) \end{cases}, \tag{1}$$

where s is the length variable along the curve. $\boldsymbol{e}_1(s), \boldsymbol{e}_2(s)$, and $\boldsymbol{e}_3(s)$ are the unit vectors that form the orthonormal basis, which is called the *Frenet–Serret frame*. $\boldsymbol{e}_1(s)$ is a unit vector that is oriented tangential to the curve at s, $\boldsymbol{e}_2(s)$ is a unit vector that indicates the direction of change in the curve at s, and $\boldsymbol{e}_3(s)$ is given by $\boldsymbol{e}_1(s) \times \boldsymbol{e}_2(s)$.

In contrast with the Frenet–Serret model, the backbone curve reflects the joint direction to model the snake robot. As shown in Fig. 2, a *backbone curve reference set* composed of $\boldsymbol{e}_r(s)$, $\boldsymbol{e}_p(s)$, and $\boldsymbol{e}_y(s)$ is defined on the curve by considering the snake robot to have the form of a continuous curve. $\boldsymbol{e}_r(s)$ is equal to $\boldsymbol{e}_1(s)$. $\boldsymbol{e}_p(s)$ is a unit vector that is oriented along the pitch axis and $\boldsymbol{e}_y(s)$ is a unit vector that is oriented along the yaw axis. These vectors comprise the basis vectors of *the backbone curve reference set*. As shown in Fig. 2, $\psi(s)$ is the twist angle of the Frenet–Serret frame and the backbone curve reference set around $\boldsymbol{e}_1(s)$, which can be obtained from $\tau(s)$ as follows:

$$\psi(s) = \int_0^s \tau(\hat{s})\mathrm{d}\hat{s} + \psi(0), \tag{2}$$

where $\psi(0)$ is an arbitrary integral constant that corresponds to the initial angle.

2) Second Step: In the first stage of the second step, we consider the curvature based on the backbone curve reference set. $\kappa_p(s)$ and $\kappa_y(s)$ are the curvatures around the pitch axis and the yaw axis in the backbone curve reference set, respectively, and can be obtained as follows:

$$\kappa_p = -\kappa(s)\sin\psi(s), \kappa_y = \kappa(s)\cos\psi(s). \tag{3}$$

Finally, the target angle of each joint is calculated using

$$\theta_i^d = \begin{cases} \int_{s_\mathrm{h}-(i-1)l}^{s_\mathrm{h}-(i+1)l} \kappa_p(s)\mathrm{d}s & (i:\mathrm{odd}) \\ \int_{s_\mathrm{h}-(i-1)l}^{s_\mathrm{h}-(i+1)l} \kappa_y(s)\mathrm{d}s & (i:\mathrm{even}) \end{cases}, \tag{4}$$

where s_h is the head position of the snake robot on the target continuous curve.

Authorized licensed use limited to: Hainan University. Downloaded on February 10,2025 at 12:26:22 UTC from IEEE Xplore. Restrictions apply.

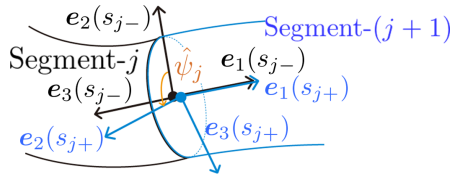

Fig. 3. Joint between segments [12].

By changing s_{h} smoothly, the region corresponds to the body of the robot in the target curve and the robot can then change its shape. This control method is called *shift control*.

B. Backbone Curve Connecting Simple Shapes

It is difficult to represent complex target forms analytically. There is also the problem that the torsion may sometimes become infinite if there are regions of zero curvature within the target form [7]. To solve these problems, we proposed a method to express the target form based on connection of simple shapes for which the curvature and the torsion are clear. Using this method, we can then design the target form intuitively. The simple shapes that are connected in this method are called *segments*. In this section, we describe how the target form can be configured by connecting these segments and thus replace the first step of the shape fitting process.

At the *connection part*, in which the segments are connected, the Frenet–Serret frame is discontinuous. Therefore, it is necessary to devise a representation of the target form. When counting from the tail-side, the j-th segment is referred to as *segment-j*($j \in \mathbb{Z}$). $s = s_j$ is the point of connection-part-j, which connects segment-j and segment-$(j+1)$, and is obtained from the length of segment-j l_j.

$$s_j = s_{j-1} + l_j. \tag{5}$$

The state of connection-part-j is shown in Fig. 3. s_{j-} and s_{j+} are the points at infinitesimal distances before and after connection-part-j, respectively. The Frenet–Serret frame, the curvature, and the torsion at s_j are represented by the corresponding values at s_{j-}.

The curvature and the torsion of segment-j are denoted by κ_j and τ_j, respectively. The curvature of the target form $\kappa(s)$ and the torsion $\tau(s)$ can be obtained as follows:

$$\kappa(s) = \kappa_j,\ \tau(s) = \tau_j \quad (s_{j-1} < s \leq s_j) \tag{6}$$

Next, we consider the twist at the connection part. As shown in Fig. 3, the angle between $\boldsymbol{e}_2(s_{j-})$ and $\boldsymbol{e}_2(s_{j+})$ around $\boldsymbol{e}_1(s_{j-})$ is denoted by $\hat{\psi}_j$. To consider this twist angle within the relationship between the Frenet–Serret frame and the backbone curve, (2) must be replaced by

$$\psi(s) \;=\; \int_0^s \tau(\hat{s})\mathrm{d}\hat{s} + \psi(0) + \sum_j \hat{\psi}_j u(s - s_j), \tag{7}$$

where $u(s)$ is the step function that has a value of 0 if $s < 0$ and 1 if $s \geq 0$. The first step of the shape fitting procedure is now replaced and thus the desired joint angles of the snake robot can be obtained using (3), (4), (6), and (7). To design the target form, we must first determine the shape of each segment and the twist angle $\hat{\psi}_j$.

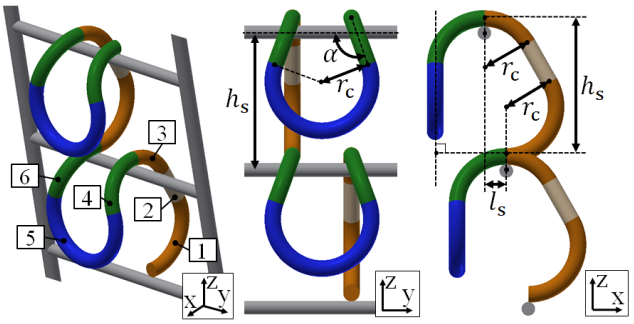

Fig. 4. Segment configuration for the ladder climbing motion.

In this paper, we use a straight line and a circular arc as the simple shapes for segments in which the curvature and the torsion are constant. In the case of a straight line, the Frenet–Serret frame and the torsion are not defined. In this study, we newly define torsion to be zero so that the straight line segments can be handled in the same way as other segments. The frame inside the straight line is defined as being equal to the frame at $s = s_{j-}$ and the torsion is zero. A circular arc, in which the curvature is constant and the torsion is zero, is defined by its radius r_j and its central angle ϕ_j. The length of a circular arc segment is calculated to be $r_j\phi_j$.

C. Shape Constraints

We consider a shape constraint condition where the target joint angle does not exceed $\theta_{\max}$. The upper limit of the absolute value of the curvature $\kappa_{\max}$ is determined to be $\kappa_{\max} = \theta_{\max}/2l$. Next, we consider the case where the shape is designed such that $\kappa(s)$ satisfies

$$|\kappa(s)| \leq \kappa_{\max}. \tag{8}$$

In this case, (3) and (4) yield

$$\begin{aligned} |\theta_i^d| \;&=\; \begin{cases} \left|\int_{s_{\mathrm{h}}+(i-1)l}^{s_{\mathrm{h}}+(i+1)l} -\kappa(s)\sin\psi(s)\mathrm{d}s\right| & (i:\text{odd}) \\ \left|\int_{s_{\mathrm{h}}+(i-1)l}^{s_{\mathrm{h}}+(i+1)l} \kappa(s)\cos\psi(s)\mathrm{d}s\right| & (i:\text{even}) \end{cases} \\ &\leq\; \int_{-l}^{l} |\kappa(s)|\mathrm{d}s \;=\; 2l\kappa_{\max} \;=\; \theta_{\max}. \end{aligned} \tag{9}$$

We can thus confirm that the absolute value of the target joint angle $|\theta_i^d|$ does not exceed $\theta_{\max}$.

III. Gait Design for Ladder Climbing

A. Basic Form

The basic form of the gait required to climb a ladder is shown in Fig. 4. In addition, a projection of part of this form on the zx-plane is shown in Fig. 5. This form consists of repeatedly connected units that are configured by combining six simple shapes. One unit corresponds to one step of the ladder. The shapes of the segments are defined using h_{s}, l_{s}, α, and r_{c}, as shown in Table I, where $n \in \mathbb{N}$ is a unit index. h_{s} and l_{s} are the vertical interval and the horizontal interval

Authorized licensed use limited to: Hainan University. Downloaded on February 10,2025 at 12:26:22 UTC from IEEE Xplore. Restrictions apply.

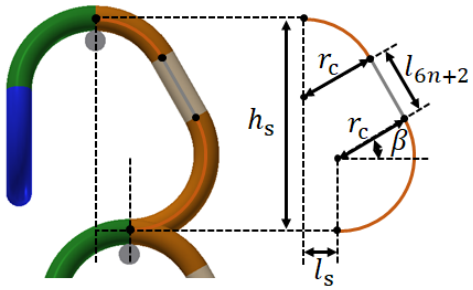

Fig. 5. Schema showing the form of the ladder climbing motion.

TABLE I

PARAMETERS OF SEGMENTS USED TO COMPOSE THE GAIT REQUIRED TO CLIMB A LADDER

seg no. j	type	parameter	$\hat{\psi}_j$
$6n+1$	circular arc	(r_j, ϕ_j)=$(r_c, \frac{\pi}{2}+\beta)$	$(-1)^n(\alpha+\frac{\pi}{2})$
$6n+2$	straight line	l_j=$(h_s-2r_c)/\cos\beta$	0
$6n+3$	circular arc	(r_j, ϕ_j)=$(r_c, \frac{\pi}{2}-\beta)$	0
$6n+4$	circular arc	(r_j, ϕ_j)=$(r_c, \frac{\pi}{2})$	$(-1)^n(\alpha-\frac{\pi}{2})$
$6n+5$	circular arc	(r_j, ϕ_j)=$(r_c, 2\alpha)$	$(-1)^{n+1}\frac{\pi}{2}$
$6n+6$	circular arc	(r_j, ϕ_j)=$(r_c, \frac{\pi}{2})$	$(-1)^n\frac{\pi}{2}$

between the steps of the ladder, respectively. These intervals are dependent on the shape of the ladder. α is the angle that is shown in Fig. 4. Increasing α makes the part that catches the step higher but also increases the required length of the snake robot per step on the ladder. r_c is the radius of all circular arcs. A smaller value of r_c means that the required length of the snake robot per step is shorter, while a larger r_c value makes the robot form smoother. The minimum value of r_c is determined based on the shape constraints shown in sub-section II-C. β in the table can be obtained based on the geometrical relationship shown in Fig. 5, as follows.

$$\beta = \arctan\left(\frac{l_s}{h_s - 2r_c}\right). \tag{10}$$

From this equation, to be able to calculate β, h_s must meet the following condition:

$$h_s > 2r_c \tag{11}$$

Shift control is used to generate the ladder climbing motion. It is possible to climb up the ladder by shifting s_h in the positive direction and to climb down the ladder by shifting s_h in the negative direction.

B. Hanging Motion

Problems arise when attempting to realize a ladder climbing motion using only shift control in its basic form. As shown in the upper part of Fig. 6, when the robot is trying to hang on the next step, it sometimes fails to reach the next step because of deflections that occur in the part that is lifted by gravity or because of approximation errors. To solve this problem, the motion is improved so that the snake robot hangs onto the next step after lifting its head to be higher than the step, as shown in the lower part of Fig. 6. To realize this motion, the shapes of segment-$6n+3$ and

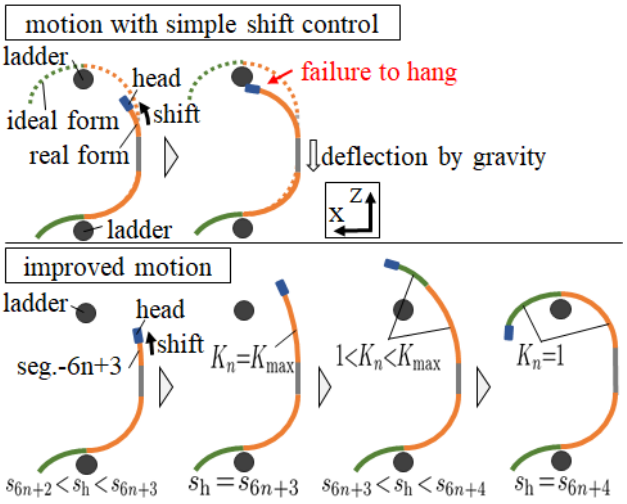

Fig. 6. Upper: Failure to hang on the next step when using simple shift control. Lower: Improved motion used to catch the next step successfully.

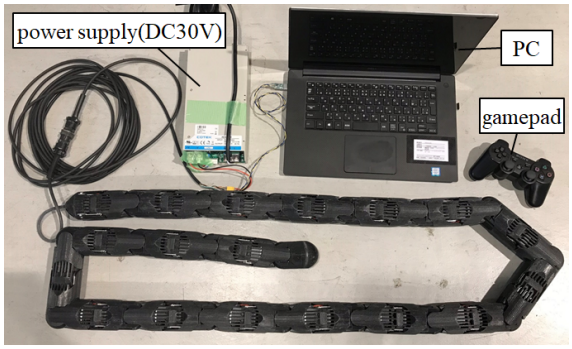

Fig. 7. Snake robot.

segment-$6n+4$ of the target form are changed in accordance with s_h, as follows.

$$(r_{6n+3},\ \phi_{6n+3}) = \left(K_n r_c,\ \frac{\frac{\pi}{2}-\beta}{K_n}\right) \tag{12}$$

$$(r_{6n+4},\ \phi_{6n+4}) = \left(K_n r_c,\ \frac{\pi}{2K_n}\right) \tag{13}$$

$$K_n = \begin{cases} \mathrm{K_{max}} & (s_{6n+2} < s_h \le s_{6n+3}) \\ \frac{\mathrm{K_{max}}(s_{6n+4}-s_h)+(s_h-s_{6n+3})}{l_{6n+4}} & (s_{6n+3} < s_h \le s_{6n+4}) \\ 1 & (\text{other}) \end{cases} \tag{14}$$

Here, K_n is the magnification of the radii of segment-$6n+3$ and segment-$6n+4$ and $\mathrm{K_{max}} > 1$ is the maximum value of K_n. l_{6n+3} and l_{6n+4}, which are the lengths of segment-$6n+3$ and segment-$6n+4$, respectively, remain constant, regardless of the value of K_n. If $\mathrm{K_{max}}$ is too high, the head then rises to a higher position and the snake becomes unbalanced.

IV. Design of the Snake Robot

The system configuration of the snake robot is shown in Fig. 7. The snake robot has a module configuration in which each module is composed of a link and a joint, as shown

Authorized licensed use limited to: Hainan University. Downloaded on February 10,2025 at 12:26:22 UTC from IEEE Xplore. Restrictions apply.

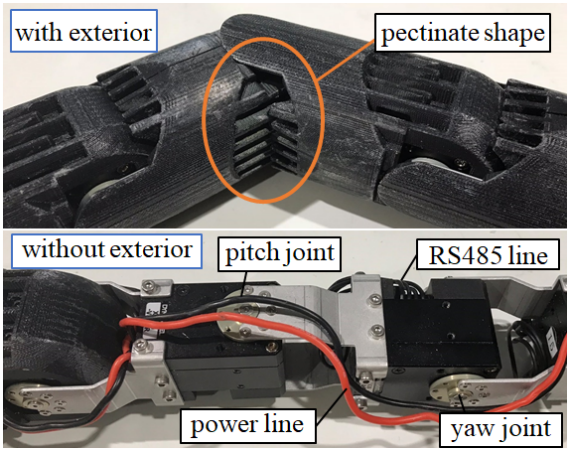

Fig. 8. Module Configuration.

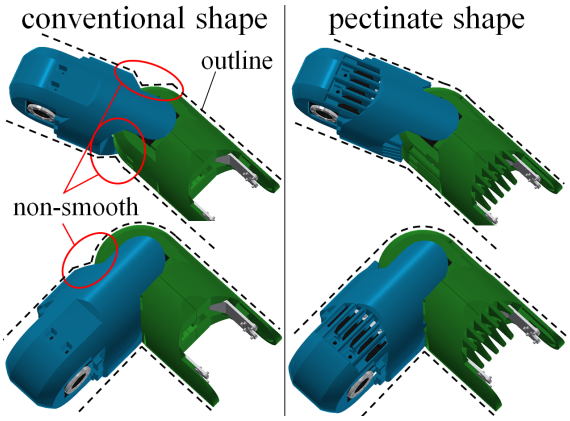

Fig. 9. Comparison of conventional and pectinate shapes.

in Fig. 8. The link length l is 70 mm, the diameter of the thickest part of the link is 56 mm, and the mass of a single module is approximately 0.15 kg. All joints have a range of motion of 180 deg., i.e., $\theta_{\max} = 90°$. The DYNAMIXEL XH430-V350-R (ROBOTIS) is used as the joint actuator and the maximum torque is approximately 4.0 Nm. The robot is composed of 36 joints. The snake robot is powered via a power cable and the target angle for each joint is sent from a computer on the operator side through an RS485 interface. It is possible to obtain information about the robot, including the joint angle and the motor current. The sampling time required to update the target joint angle is 20 ms. The operator can control the robot ' s operations via a gamepad.

The maximum curvature $\kappa_{\max}$ that this snake robot can achieve is 0.0112 mm^{-1}, and thus the minimum value of r_c is 89.1 mm. Therefore, from (11), to enable use of this snake robot, the vertical interval between the steps of the ladder must be greater than 178.2 mm. This value is small enough to allow this snake robot to be applied to a real ladder.

To ensure that the snake robot can move without becoming stuck in the environment, it is important that its exterior body surface is smooth. We therefore developed a snake robot that had a smooth exterior body surface by giving the links

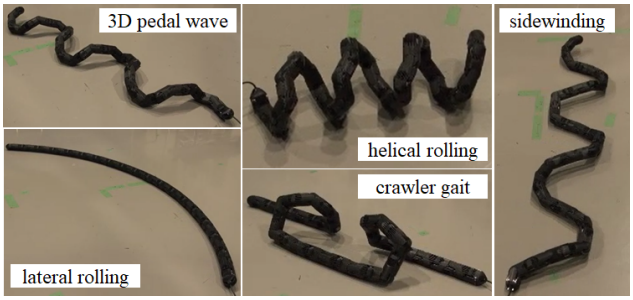

Fig. 10. Experimental results showing realization of various gaits.

the pectinate shape that is shown in the upper side of Fig. 8. A comparison between the conventional shape and the pectinate shape that we proposed is shown in Fig. 9. The broken lines in Fig. 9 indicate the approximate outline of the robot. The snake robot *Aiko* [15] that was developed at the Norwegian University of Science and Technology (NTNU)/SINTEF Advanced Robotics Laboratory and the *SEA Snake* [16] that was developed by D. Rollinson et al. have almost smooth surface shapes, but this is not sufficient for our purposes because of the nonsmooth parts shown on the left side of Fig. 9. Because this part has a concave shape, it can become caught within the environment. In the conventional design, if this nonsmooth part is filled by simply extending the exterior to make the shape smooth, the exterior parts interfere with each other and the range of motion of the joint thus decreases. However, in the proposed design shown on the right side of Fig. 9, the surface shape is smoothed using the pectinate part, and this part does not affect the bending of joints. The interval between the teeth of the comb structure is 3 mm, which means that grains larger than 3 mm do not get inside the robot. This thickness of the comb structure is designed to provide sufficient strength, and it is possible to make the comb thinner by simply using a stronger material. The exterior of the link is fabricated using a 3D printer, and the material used is acrylonitrile butadiene styrene (ABS).

The exterior also has the function of protecting the cable. In addition to covering the cable, the exterior guides the cable to pass on the joint axis and the load acting on the cable due to the bending of the joint is thus reduced.

V. Experiment

A. Variety of Snake Gaits

Experiments were performed to verify the basic functionality of the developed snake robot. As shown in the figure, a variety of gaits, including the 3D pedal gait [17], the lateral rolling gait [11], the helical rolling gait [11], the crawler gait [12], and sidewinding [3], were realized using the developed snake robot. The smooth surface shape can potentially be used in the various gaits.

B. Ladder Climbing

Experiments were performed to verify the effectiveness of the both proposed climbing gait and the developed snake

Authorized licensed use limited to: Hainan University. Downloaded on February 10,2025 at 12:26:22 UTC from IEEE Xplore. Restrictions apply.

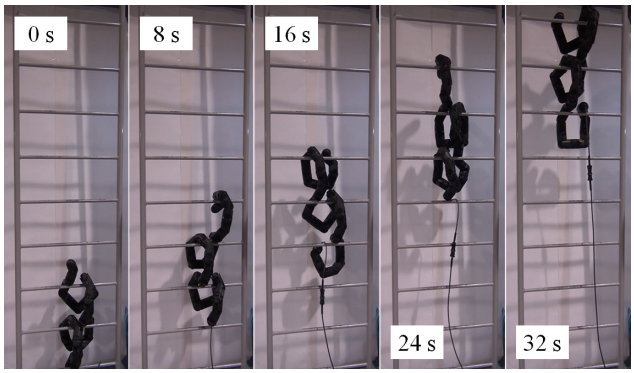

Fig. 11. Experimental results for snake robot climbing a vertical ladder.

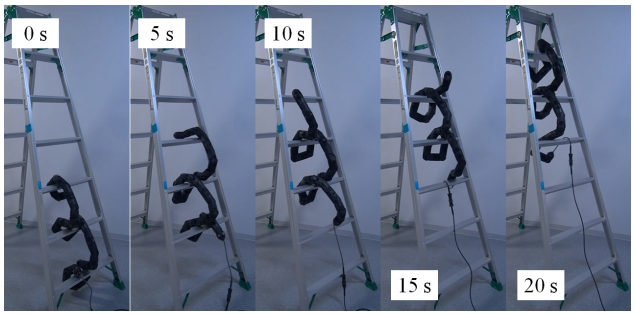

Fig. 12. Experimental results for snake robot climbing an inclined ladder.

robot. We performed two experiments in which the snake robot climbed a vertical ladder and a ladder that was inclined at 75°. The parameters h_{s} and l_{s} are 250 mm and 0 mm in the experiment on the vertical ladder and 295 mm and 79 mm in the experiment on the inclined ladder, respectively. In both experiments, r_{c} was set to the minimum value of 89.1 mm. α and $\mathrm{K}_{\max}$ were adjusted through a trial and error process, and were set to 115°. and $\mathrm{K}_{\max}$, respectively. Proposal of a suitable parameter optimization method is a task for future work.

The experimental results for climbing of the vertical ladder and the inclined ladder are shown in Fig. 11 and Fig. 12, respectively. The operator executed the shift control process only, and the hanging motion was executed in accordance with (12)–(14) along with the shift control process. The speed at which s_{h} changes to perform the shift control is constant at 0.18 m/s. In both experiments, the snake robot was able to climb the target ladders successfully. Because its exterior body surface was smooth, the snake robot was able to slide on the steps without becoming stuck. Note that the cable connected to the snake robot did not become caught in the ladder.

VI. Conclusions

We proposed a method to allow a snake robot to climb a ladder. The target form of the proposed gait was designed by connecting simple shapes such as straight lines and circular arcs. This target form can be adjusted easily using four types of parameters and the climbing motion is generated using a combination of shift control and hanging motion. In addition, we developed a novel snake robot that has a smooth exterior body surface by using a pectinate-shaped part on the link. We performed experiments to verify the effectiveness of the proposed gait and demonstrated that the snake robot could climb both a vertical ladder and an inclined ladder.

Kinematic and dynamic analyses of the proposed gait will form part of our future work. In addition, for use in unknown environments, it will be necessary for the snake robot to be able to climb ladders with unknown shapes. Determination of a method to allow the snake robot to measure the shape of a ladder and then climb it automatically will also form part of our future work.

References

[1] S. Hirose, *Biologically Inspired Robots: Snake-Like Locomotor and Manipulator*, Oxford, U.K.: Oxford University Press, 1987.
[2] M. Tanaka and K. Tanaka, "Control of a snake robot for ascending and descending steps," *IEEE Trans. Robot.*, vol. 31, no. 2, pp. 511-520, Apr. 2015.
[3] M. Tesch, K. Lipkin, I. Brown, R. Hatton, A. Peck, J. Rembisz, and H. Choset, "Parameterized and Scripted Gaits for Modular Snake Robots," *Advanced Robotics*, vol. 23, no. 9, pp. 1131–1158, 2009.
[4] D. Rollinson and H. Choset, "Pipe Network Locomotion with a Snake Robot," *Journal of Field Robotics*, vol. 33, no. 3, pp. 322—336, 2016.
[5] R. L. Hatton and H. Choset, "Generating gaits for snake robots: annealed chain fitting and keyframe wave extraction," *Auton. Robot*, vol. 28, no. 3, pp. 271–281, 2010.
[6] P. Liljebäck, K. Y. Pettersen, Ø. Stavdahl, and J.T. Gravdahl, "A 3D Motion Planning Framework for Snake Robots," *Proc. IEEE/RSJ Int. Conf. on Intelligent Robots and Systems* 2014, pp. 1100-1107.
[7] H. Yamada and S. Hirose, "Study on the 3D Shape of Active Cord Mechanism," *Proc. IEEE Int. Conf. on Robotics and Automation*, 2006, pp. 2890–2895.
[8] H. Yamada and S. Hirose, "Study of Active Cord Mechanism — Approximations to Continuous Curves of a Multi-joint Body—," *J. of the Robotics Society of Japan*, vol.26, no.1, pp.110–120, 2008. (in Japanese with English Summary)
[9] T. Kamegawa, T. Baba, and A. Gofuku, "V-shift control for snake robot moving the inside of a pipe with helical rolling motion," *Proc. IEEE Int. Symp. on Safety, Security, and Rescue Robotics*, 2011, pp. 1–6.
[10] T. Kamegawa, T. Baba, and A. Gofuku, "Proposal of helical wave propagate motion for a snake robot to across a branch on a pipe," *Proc. IEEE/SICE Int. Symp. on System Integration*, 2016, pp. 821–826.
[11] W. Zhen, C. Gong, and H. Choset, "Modeling Rolling Gaits of A Snake Robot," *Proc. IEEE Int. Conf. on Robotics and Automation*, 2015, pp. 3741–3746.
[12] T. Takemori, M. Tanaka, and F. Matsuno, "Gait Design of a Snake Robot by Connecting Simple Shapes," *Proc. IEEE Int. Symp. Safety, Security Rescue Robot.*, 2016.
[13] T. Takemori, M. Tanaka, and F. Matsuno, "Gait Design for a Snake Robot to Climb a Ladder," *The 2nd Int. Symp. on Swarm Behavior and Bio-Inspired Robotics.*, 2017, pp. 89–92.
[14] G. S. Chirikjian and J. W. Burdick, "The Kinematics of Hyper-Redundant Robot Locomotion," *IEEE Trans. Robot. Autom.*, vol. 11, no. 6, pp. 781–793, Dec. 1995.
[15] A. A. Transeth, R. I. Leine, C. Glocker, and K. Y. Pettersen, "Snake robot obstacle-aided locomotion: Modeling, simulations and experiments," *IEEE Trans. on Robotics*, vol. 24, pp. 88–104, 2008.
[16] D. Rollinson, Y. Bilgen, B. Brown, F. Enner, S. Ford, C. Layton, J. Rembisz, M. Schwerin, A. Willig, P. Velagapudi, and H. Choset, "Design and Architecture of a Series Elastic Snake Robot," *Proc. IEEE/RSJ Int. Conf. on Intelligent Robots and Systems*, 2014, pp. 4630–4636
[17] H. Ohno and S. Hirose, "Design of slim slime robot and its gait of locomotion," *Proc. IEEE/RSJ Int. Conf. on Intelligent Robots and Systems*, 2001, pp. 707–715.

Authorized licensed use limited to: Hainan University. Downloaded on February 10,2025 at 12:26:22 UTC from IEEE Xplore. Restrictions apply.